13th World Conference on Earthquake Engineering
Vancouver, B.C., Canada
August 1-6, 2004
Paper No. 976

EXPERIMENTAL RESEARCH ON LOAD RESISTANCE PERFORMANCE OF CFT COLUMN/FLAT PLATE CONNECTION

Hiroki Satoh [1] and Kazushi Shimazaki [2]

SUMMARY

Buildings that are composed of coupled shear walls with dampers, CFT columns, and flat plate slabs are one of the types of buildings that can be reused, with low repair cost, after an earthquake. To evaluate the behavior of the newly designed CFT column/flat plate connection, three series of experimental studies were carried out: 1) lateral loading tests for interior column/slab connections, 2) element specimens for punching shear strength, and 3) element specimens for torsional strength.
Strength capacity and load-deflection behavior of the CFT column/flat plate connection were examined using macro models, and a design procedure was proposed.

INTRODUCTION

The current objective of earthquake resistant design is not only to protect life in very severe earthquakes, but also to enable the reuse of buildings, at a low repair cost, after an earthquake. A building system such as the one shown in Figure 1 composed of "coupled shear core walls with dampers", CFT (concrete filled steel tube) columns, and flat plate slabs is one of the types of buildings that can meet such requirements. This system is expected to reduce the gross building weight, extend the span, enhance workability, and provide freedom of space. In this study, an eight-story building with 300-mm slab thickness and 10-m spans was assumed as the prototype building.

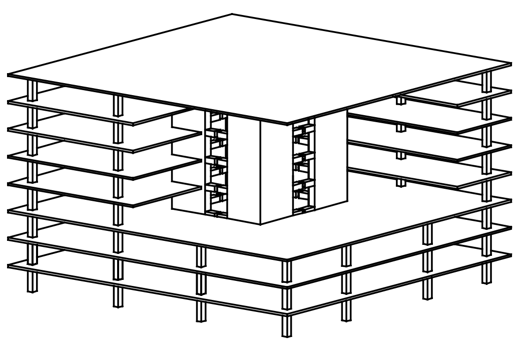

Figure. 1 : Prototype building

[1] Kanagawa University, Japan; Email: satouh16@kanagawa-u.ac.jp
[2] Kanagawa University, Japan; Email: shimak19@kanagawa-u.ac.jp

As the floor load should be supported even under conditions of large deformation at the CFT column/flat plate connection, punching shear failure must be avoided. To evaluate the strength capacity and load-deflection behavior of the connections of CFT column/flat plate slab, three series of experimental studies were carried out: 1) lateral loading tests for interior column/slab connections, 2) element specimens for punching shear strength, and 3) element specimens for torsional strength. After examining the test results, a design method for the connection was proposed.

Common Design Method

In the design of the reinforced concrete flat slab structure complying with AIJ standard for structural design of RC structures (AIJ RC standard), punching shear failure occurs as a result of the combination of shear force around the column, moment and shear force at the front and back of the column, and torsional moment at the column side. Around the connection, the moment, which is not consistent in the slab, is transferred from the flat slab to the column. This moment is defined as the "unequal moment". Shear failure is calculated using Eq. (1) as the sum of the ratio of design shear force to strength, plus the design unequal moment to strength, which should be less than one[1,2].

$$\frac{\alpha V_u}{V_0} + \frac{M_u}{M_0} \leq 1 \quad \cdots\cdots\cdots\cdots \quad (1)$$

where

V_u: design shear force
V_0: shear force strength
α : additional factor by vertical vibration
M_u: design unequal moment
M_0: unequal moment strength

Design shear force V_u and design unequal moment M_u are the sum of the values at vertical load and horizontal force. Shear force strength V_0 is the value of the critical section slab as effective width. Unequal moment strength M_0 is as follows:

$$M_0 = M_m + M_s + M_t \quad \cdots\cdots\cdots\cdots \quad (2)$$

where

M_m: moment strength at front and back of column face
M_s: moment strength at front and back of column face by shear force
M_t: torsion moment strength at side of column face

It is necessary to evaluate the design force at vertical and horizontal loading. As the stiffness degrades with cracking of the slab, which comes in from the initial stage, the load-deformation relation must be evaluated in order to determine the design force. Punching shear strength must also be examined after horizontal loading.

EXPERIMENTAL RESEARCH

Outline of Tests

The experiment consisted of three series of tests: frame test (Fp series, Fig. 2a), push-out element test (Ps series, Fig. 2b), and torsion element test (Ts series, Fig. 2c). The specimen for the Fp series assumed the part of an intermediate story and center position of the column/flat plate frame shown in Fig. 1. The slab edge of the specimen is in the center of the span. The column end of the test specimen is the middle of the story. The scale was made to be about 1/2.24. The Ps series specimens were taken from the slab part

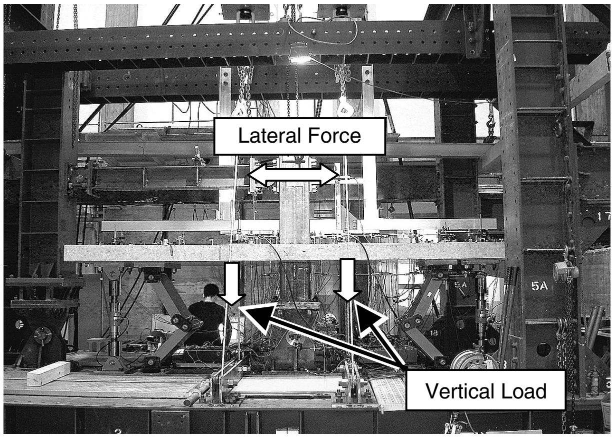

Fig. 2(a) : Fp series test

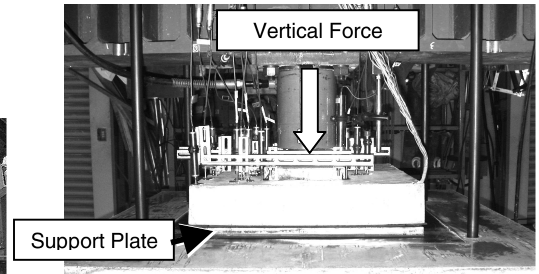

Fig. 2(b) : Ps series test

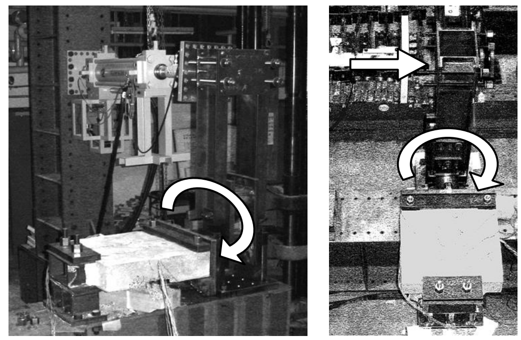

Fig. 2(c) : Ts series test

around the column with additional column width from the column face as shown in Fig. 2(b), in which punching shear failure was assumed. The Ts series specimens are part of the column side as shown in Fig. 2(c), in which the torsion affects.

The connection plate, which is welded to the diaphragm of CFT steel pipe, and the web reinforcement of H-shape steel embedded in flat plate slab are connected by a high-strength bolt as shown in Fig. 3. This connection plate is also expected to resist punching shear stress. The diaphragm functions as the continuity plate. Slab reinforcements, which do not penetrate the column, create a 180° hook at the front of the column surface.

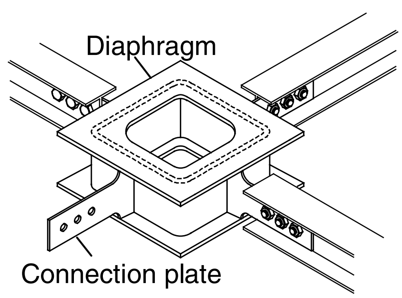

Fig. 3 : CFT column-flat plate connection

Fp series test

The design of the prototype structure was based on the AIJ RC standard. From the results of preliminary analysis of the prototype building, the column/flat plate frame was assumed to resist 20% of the story-shearing force during an earthquake. The test specimens were designed to have the same ratio of design force to strength. Details of the test specimens are shown in Fig. 4. The test parameters consisted of the connection plate type, amount of reinforcing bars, shear reinforcement, vertical load, and unconnected part around the column face. The list of parameters is shown in Table 1. The material characteristics used for the specimens are shown in Table 2.

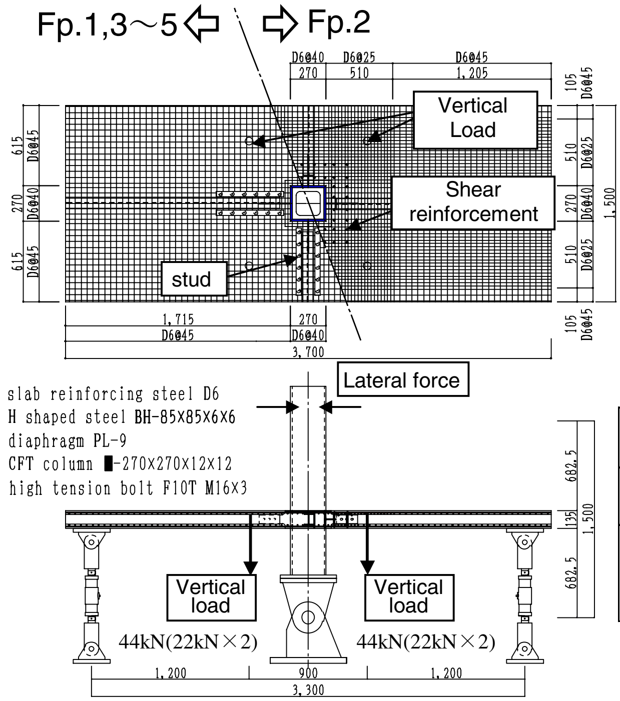

Fig. 4 : Detail of specimens

Table. 1 : Test parameter of Fp series

Test specimen	Connection plate	Shear reinforcement	Connection face	Vertical load
Fp.1	6×65	—	Full face	15 kN/m²
Fp.2	6×65 (Cruciform)	D6@90		
Fp.3	6×60	φ9@90 (Stud)		—
Fp.4			Front and back	
Fp.5			Side	

Table. 2 : Material properties of Fp series

Concrete		Compressive strength (N/mm²)	Tensile strength (N/mm²)	Young's modulus (N/mm²)	Steel materials		Yield stress (N/mm²)	Ultimate strength (N/mm²)
Fp1,2	Fc35	69.1	—	3.24×10^4	D6	SD295	385	559
					PL-6	SS400	432	582
					PL-9		357	548
Fp.3,4	Fc35	44.0	3.4	3.22×10^4	D6	SD295	380	521
					studφ9	SR295	467	808
					PL-6	SS400	460	600
					PL-9		367	560
					PL-12		362	554

The test specimen was supported at the slab edge by a pin/roller configuration and at the column base by pinned support as shown in Fig. 4. An actuator at the column top was applied for horizontal force. Vertical load was continuously applied for the Fp-1 and Fp-2 specimens. Loading cycles were 1 time at R = 1/1000, two times at 1/500 and 1/200, 6 times at 1/100, 2 times at 1/67, 1/50 and 1/33, and 1 time at 1/20.

Figure 5 shows the final crack pattern of the Fp-3 and Fp-5 specimens. The critical cross-section position, at which the bending moment reaches the maximum, was estimated from the crack width and the strain distribution of the reinforcing bars. This position is drawn in the figure. The critical cross section extends in a 45° direction from the column face, and changes parallel to the slab width direction for the Fp-3 and Fp-4 specimens. For Fp-5, it is almost parallel to the column width.

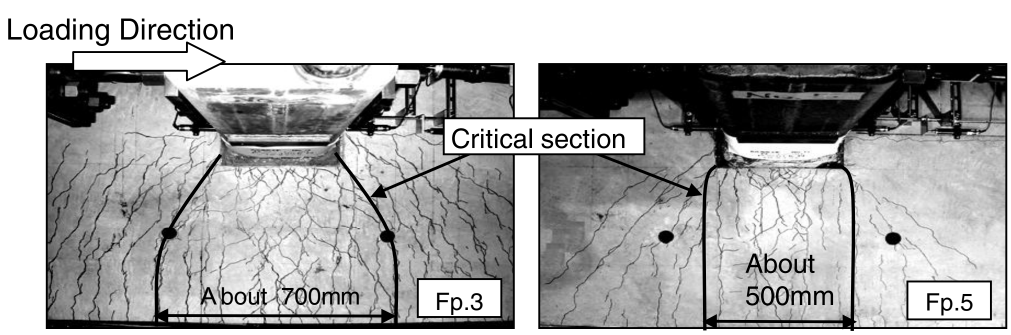

Fig. 5 : Crack Pattern

Figure 6 shows the horizontal force-deformation relationship. For Fp-1, Fp-2 and Fp-3, the slab reinforcement yielded in the full slab width, and the maximum horizontal resistance is determined by the bending capacity of the slab. No punching shear failure occurred in these specimens. For Fp-4, shear crack was observed 45° diagonally from the column face with some concrete crush. For Fp-5, the largest resistant force developed from torsion yield at the column side. Comparing Fp-1 and Fp-3, there is little effect of vertical load. The value of horizontal force obtained by inverse calculation of Eq. (1) with bending moment strength and punching shear strength (using real strength) in accordance with the AIJ RC standard is also shown in Fig. 6. The calculated value takes unequal moment M_u as the value calculated from horizontal force and column length, and design shear force V_0 as the vertical load (for Fp-1 and Fp-2). The experimental strength is about 1.11 times the calculated strength.

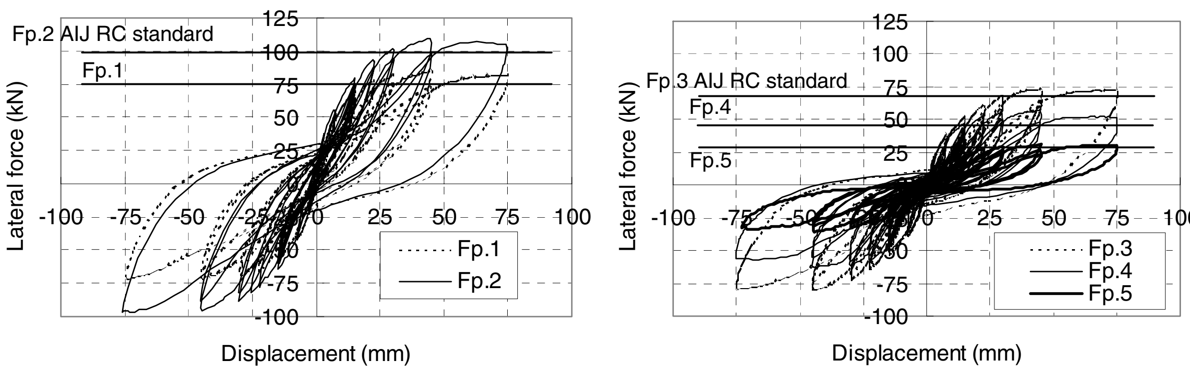

Fig. 6 : Load-Deflection Relationship

From the Fp series tests, the following conclusions were obtained:

1. The punching shear strength can be evaluated by the AIJ RC standard equation, erring on the safe side.
2. The critical cross-section position was grasped, acting shear force and bending moment at the front and back of the column face, and torsional moment at the column side.

Ps series test

Figure 7 shows details of the test specimens. The parameters consisted of concrete strength, existence of studs, effect of connection plate, and effect of bending crack at the specified deformation level as listed in Table 3. The material characteristics are shown in Table 4.

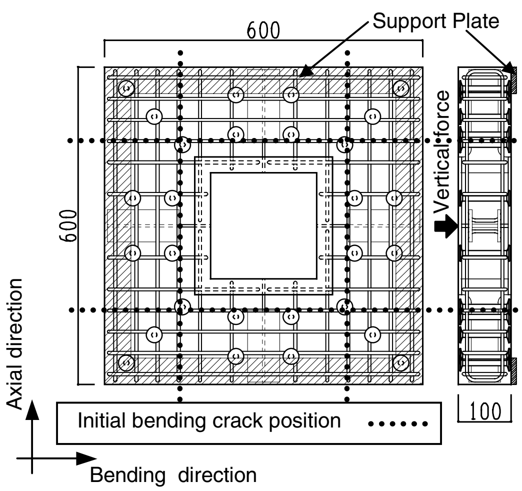

Fig. 7 : Detail of specimens

Table. 3 : Test parameters of Ps series

		H shape steel	Stud	Initial bending crack (Story deformation angle)	Reinforcing bars
Ps.1	Fc36	–	–	–	–
Ps.2					D6@40
Ps.3	Fc24	60×60×4×4			
Ps.4	Fc36				
Ps.5	Fc60				
Ps.6	Fc36	90×60×4×4			
Ps.7		–	ϕ9@75		
Ps.8		60×60×4×4			
Ps.9				1/200	
Ps.10				1/100	
Ps.11				1/20	
Ps.12		60×60×4×4*	–	–	
Ps.13		–			UD6@40

* Only web of H shape steel was connected

Table. 4 : Material properties of Ps series

	Concrete	Compressive strength (N/mm^2)	Tensile strength (N/mm^2)	Young's modulus (N/mm^2)	Steel materials		Yield stress (N/mm^2)	Ultimate strength (N/mm^2)
Ps series	Fc24	21.4	2.6	2.56×10^4	D6	SD295	463	567
					ϕ9	SR295	467	808
	Fc35	45.1	3.5	2.70×10^4	UD6	Ulbon785	952	1030
					PL-4	SS400	374	436
	Fc60	57.2	3.9	3.20×10^4	PL-6		460	600
					PL-12		362	554

Vertical force was applied by hydraulic jack at the column position supported by the support plate at the outer slab. The rotation of the slab edge was not restricted. The shear span ratio was about 1.3. The push-out test for the Fp series specimens was also conducted after the horizontal loading test.

For specimens Ps-3, 4, 5, 6, 8, 9, 10 and 11, which have the embedded H steel, crack was observed at the upper part of the H steel first, and radial cracks were observed as bending cracks. Same radial cracks developed bending shear crack with increased load. In the H-steel section, shear crack was observed diagonally from the H-steel flange. For specimens Ps-1, 2, 7 and 13, which do not have embedded H steel, bending crack was observed spreading from the diaphragm center in the diagonal direction first, and then radial cracks were observed. The crack situation is shown in Fig. 8.

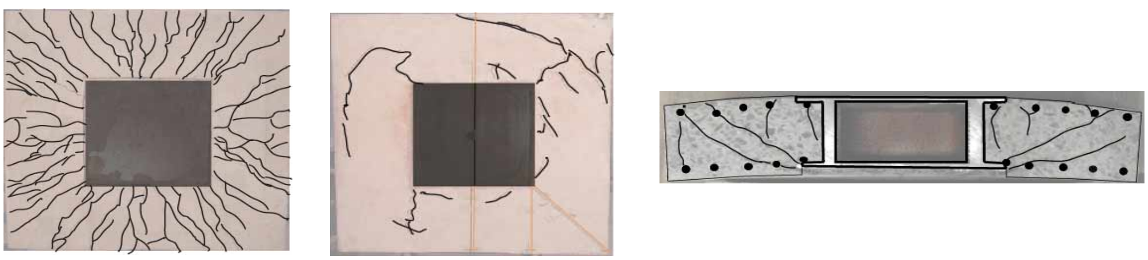

Top bottom section

Fig. 8 : Ps 8 Crack pattern

The maximum strength, shown as the sum of shear force of the connection plate, studs and concrete, is shown in Fig. 9 for all specimens. Shear force of the studs and connection plate is estimated from each strain history. Shear force of the concrete is calculated by deducting the shear force of the connection plate and studs from the total force. The ratio of shear stress of concrete to the square root of concrete compressive strength is defined as shear stress intensity coefficient ${}_c\alpha$, and is shown in the same figure. According to ACI[3], ${}_c\alpha = 0.33$ when only the concrete section is effective, and ${}_c\alpha = 0.165$ when shear reinforcement is also effective. All tested results of ${}_c\alpha$ exceed 0.165 except Ps-1, which does not have the reinforcing bar.

In the push-out test for Fp-4 and Fp-5, the critical section is at the support plate position and at a 45° line from the bonding surface, and shear fracture was observed. The Fp-3 specimen did not demonstrate failure up to the equipment limits. The studs yielded in the Fp-4 and Fp-5 specimens, but did not yield in the Ps series specimens.

The following results were obtained from the push-out tests:
1. The studs resisted push-out force.
2. The connection plate worked to resist shear force.
3. Shear strength of the concrete could be evaluated by ACI standards, erring on the safe side.

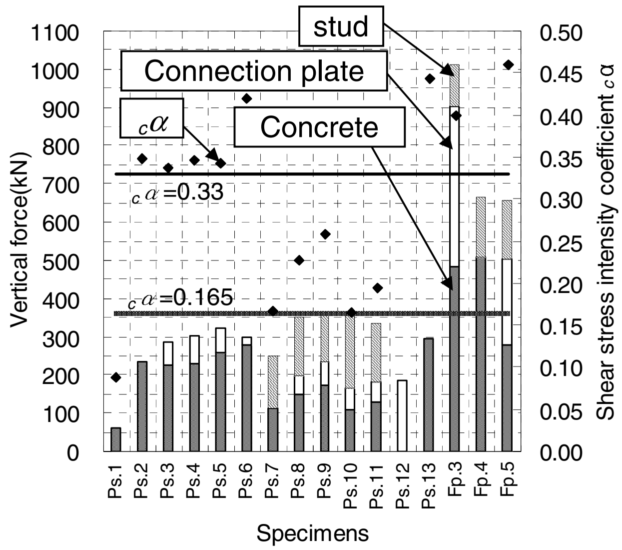

Fig. 9 : Test results of Ps series

Ts series test

Test specimens were designed to be about 1/2.24 of the prototype building, as shown in Fig. 10, which includes details of the bar arrangement. The slab width is about 2.2 times that of the column at 600 × 600 × 135 (mm).

The test parameters consisted of concrete strength, existence of studs, existence of reinforcing bars in the axial direction and bending direction, existence of H steel buried in the slab, existence of initial bending crack, and column width as shown in Table 5. The material characteristics are shown in Table 6. The specimens were fixed at the CFT section part, and torsional moment was given to the edge of the far-side slab from the column using a loading arm by actuator.

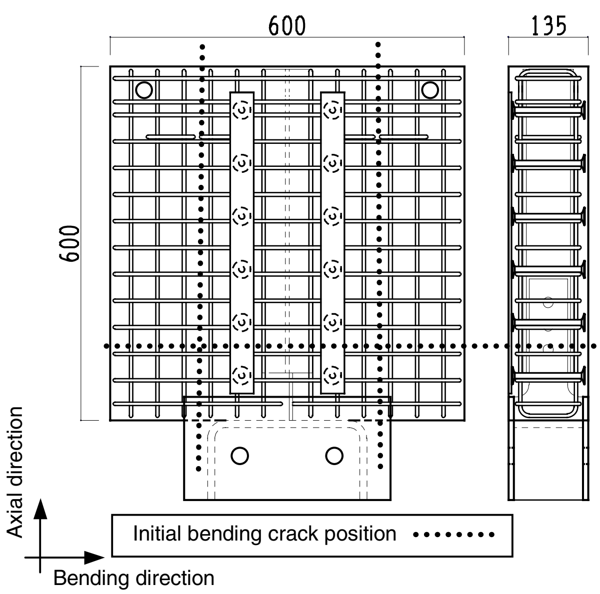

Fig. 10 : Detail of specimens

Table. 5 : Test parameters of Ts series

		Stud	Reinforcing bars		Embedded H shape steel	Initial bending crack	Width of CFT (mm)
			Axial Direction	Bending direction			
Ts.1	Fc24	-	-	-	-	-	270
Ts.2	Fc36						
Ts.3	Fc60						
Ts.4	Fc36	φ9@90					
Ts.5		-	D10@45				
Ts.6			-		85×85×6×6		
Ts.7				D10@45	-		
Ts.8		φ9@90	D10@45		85×85×6×6		
Ts.9						Axial Direction	
Ts.10						Bending direction	
Ts.11				*		-	
Ts.12		-	-	-	-		150

* Bending direction reinforcing bars was concentrated near the joint.

Table. 6 : Material properties of Ts series

	Concrete	Compressive strength (N/mm^2)	Tensile strength (N/mm^2)	Young's modulus (N/mm^2)	Steel materials		Yield stress (N/mm^2)	Ultimate strength (N/mm^2)
Ts series	Fc24	40.2	2.9	2.28×10^4	D6	SD295	374	523
					ϕ9	SR295	467	808
	Fc35	47.1	3.8	2.26×10^4	UD6	Ulbon785	952	1030
					PL-6	SS400	460	600
	Fc60	57.2	3.9	3.20×10^4	PL-9		367	560
					PL-12		362	554

The first crack was observed at about 7.2 kNm from the center of the diaphragm. The crack patterns are about 45° for the specimens without rebars. For the one-direction reinforced specimen, cracks tended to grow along the reinforcing bar. For specimens with rebars in both directions, the crack lines increased parallel to the first crack. The crack situation is shown in Fig. 11.

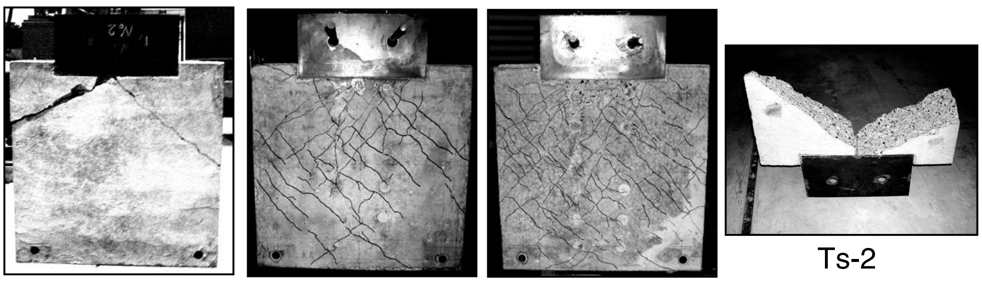

Ts-2 Ts-8 Ts-10 Ts-2

Fig. 11 : Crack pattern

Specimens Ts-1 to 7 showed the maximum strength just after the first crack. Specimens Ts-1, 2, 3, 4 and 12, which did not have reinforcement bars, degraded in strength rapidly after the first torsion crack. For specimens Ts-5, 6, and 7, which had reinforcing bars or H steel, deformation increased, retaining the strength after cracking. For specimens Ts-8 to 11, the rigidity degraded after the torsion crack, and the strength increased through the reinforcing effect of the hoop, H steel, bending reinforcing bar, axial reinforcing bar, and studs.

Figure 12a shows the maximum strength of each test specimen and strength in repetition. The calculated relation of effective width-strength using the theory of elasticity, plasticity, oblique bending and "Concrete Specifications" method[4] are shown in Fig. 12b. From Fig. 12b, the first crack strength becomes close to the value of the theory of plasticity equation with the effective width of the column width. The value of the elasticity equation also shows a close value. The maximum strength of the bidirectional reinforced test specimens (Ts-8 through 11) is close to the value calculated by the "Concrete Specifications" equation with the overall slab width as effective width. Table 7 shows the comparison of experimental results and calculated values of the torsional stiffness in the torsional moment-rotation relation. The calculated initial stiffness is obtained by the theory of elasticity using the column width as effective width. It agrees with the experimental result. The post-crack stiffness is calculated with the effective width as the column width for Case 1, and as the slab width for Case 2. The stiffness degrading rate α is calculated by the Hsu equation[5] shown in the following Eq. (3). The value of Case 2 agrees with the experimental value.

$$\alpha = 0.021 \ (p_v + p_l) \quad \cdots\cdots\cdots\cdots\cdots\cdots\cdots \quad (3)$$

where p_v is the axial reinforcement ratio and p_l is the lateral reinforcement ratio.

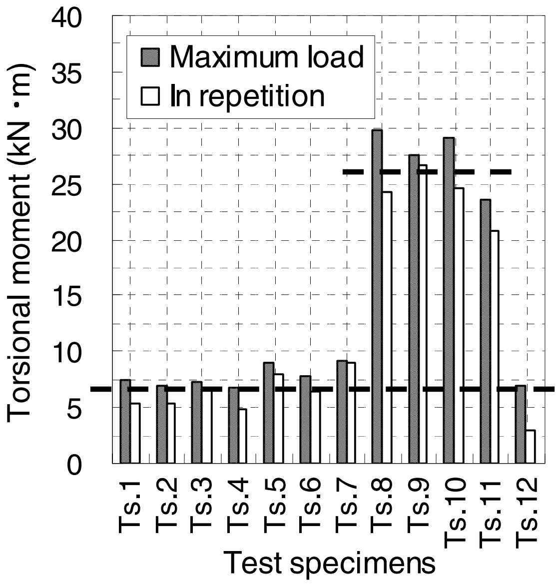

(a) Maximum strength and strength in repetition

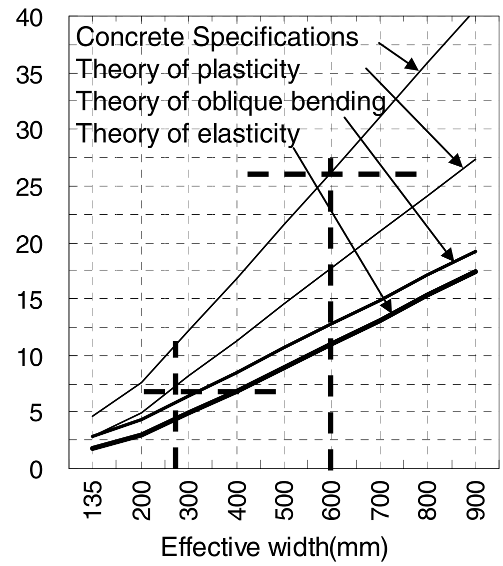

(b) Torsional moment-effective width Relationship

Fig. 12 : maximum strength of each test specimen and strength in the repetition

Table.7 : comparison of experimental results and calculated values of torsional stiffness

	Torsional stiffness [kN・m/(rad/m)]				
	Slab			Connection	
	Initial ($\times10^3$)	Stiffness regarding rate: Post-crack stiffness	Stiffness regarding rate: In repetition	Initial ($\times10^2$)	Post-crack stiffness regarding rate
Ts.1	2.72	-	-	3.18	-
Ts.2	2.30	-	-	3.11	-
Ts.3	2.67	-	-	2.95	-
Ts.4	2.17	-	-	2.93	-
Ts.5	2.78	-	-	5.93	-
Ts.6	2.15	-	-	3.17	-
Ts.7	2.52	-	-	3.83	-
Ts.8	2.37	0.11	0.05	3.55	0.65
Ts.9	1.32	0.19	0.14	2.78	0.78
Ts.10	1.92	0.14	0.07	2.48	0.72
Ts.11	2.19	0.12	0.11	2.96	0.71
Ts.12	3.57	-	-	1.13	-
No.13	3.14	-	-	2.64	-
Calculation 1	2.03	0.054	-	-	-
Calculation 2	2.03	0.134	-	-	-

Effective width for calculation
Initial torsional stiffness
Calculation1,2 : column width(270mm)
Post-crack torsional stiffness
Calculation1 : column width (270mm)
Calculation2 : slab width (600mm)

The main conclusions obtained from the Ts series tests are as follows:

1. The initial stiffness and the first crack strength can be approximately estimated using the theory of elasticity with the column width as effective width.
2. The post-crack stiffness can be estimated by applying the stiffness reduction factor by Hsu to the theory of elasticity.
3. The effect of slab reinforcement for the torsion can be estimated according to the “Concrete Specifications” method.
4. The effective width of torsion increases after the crack, and the effective width can be applied to estimate the stiffness and strength.

DESIGN METHOD

Punching shear strength

From the Fp and Ps series test results, to examine the punching shear strength by Eq. (1), shear strength V_0 and unequal moment strength M_0 can be calculated using the following equations:

$$V_0 = {}_sV + {}_cV + {}_{st}V \quad \cdots\cdots\cdots \quad (4)$$

$$M_0 = {}_cM_m + {}_cM_s + {}_sM_s + {}_cM_t \quad \cdots\cdots\cdots \quad (5)$$

where

- V_0: shear force strength
  - ${}_sV$: shear strength of connecting plate
  - ${}_cV$: shear strength of concrete
  - ${}_{st}V$: shear strength of stud
- M_0: unequal moment strength
  - ${}_cM_m$: moment transferred at front and back of column face
  - ${}_cM_s$: moment by shear force of concrete at front and back of column face
  - ${}_sM_s$: moment by shear force of connecting plate at front and back of column face
  - ${}_cM_m$: torsional moment at side of column

Load-deflection relation

A macro model was developed using the critical cross section around the joint from experimental results of the Fp and Ts series tests. This model consists of two slab parts, at the longitudinal column face and at the column side. The slab at the front and back of the column was modeled as a virtual beam with the column width size as shown in Fig. 13. The side slab was modeled as a torsion slab with the width of the critical cross section. The torsion slab was assumed to resist torsional forces by shear force and moment of slab replaced with the virtual beam at the unit width, as shown in Fig. 13.

For the virtual R/C beam, flexural crack M_c and yield strength M_y are calculated by approximate Eqs. (6) and (7), and the stiffness reduction factor α_y (Secant modulus at yield point/initial stiffness) is obtained by experimental Eq. (8)[1].

$$M_c = 0.56\sqrt{\sigma_B}Z \quad \text{(units: N, mm)} \quad \cdots\cdots\cdots\cdots\cdots\cdots\cdots \quad (6)$$

$$M_y = 0.9 a_t \sigma_y d \quad \cdots\cdots\cdots\cdots\cdots\cdots\cdots \quad (7)$$

$$\alpha_y = (0.043 + 1.64 n p_t + 0.043 a/d)(d/D)^2 \quad \cdots\cdots\cdots\cdots\cdots\cdots\cdots \quad (8)$$

where σ_B is concrete strength in N/mm^2, Z is section modulus, a_t is area of longitudinal tension reinforcement, σ_y is yield strength of steel, d is distance from extreme compression fiber to centroid of tension reinforcement, p_t is steel ratio, n is modular ratio, D is height of beam, and a is shear span length (M/Q).

The torsion slab part with the effective width of the critical cross section is divided into the unit width as well as the virtual beam, and the transmission of torsional forces between unit widths is set from the experimental results of the Ts series tests. Initial stiffness is calculated by theory of elasticity with the column width as effective width. The post-crack stiffness is calculated using the critical cross-section width as the effective width, and the stiffness degrading coefficient is taken by Hsu's equation.

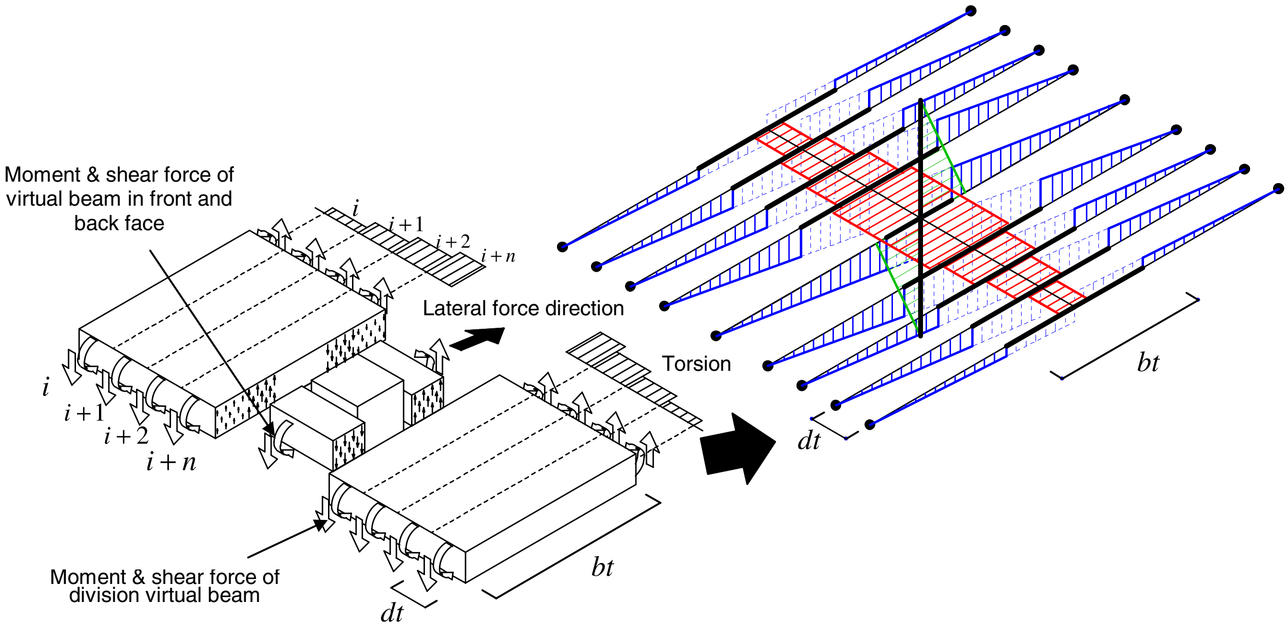

Fig. 13 : Macro model

The comparison of analytical results and experimental results is shown in Fig. 14. For the Fp-4 specimen, although the column side is not connected, the effective width of the torsion slab is larger than the width of the unconnected part, and torsional forces can transfer to the central virtual beam from out of the column width as shear force, and transfer to the column as an unequal moment by shear force. For the Fp-5 specimen, the effective width is small, because the front and back of the column have not been connected, and torsional forces are transmitted only in the direct column side. Analytical results and experimental values show good agreement.

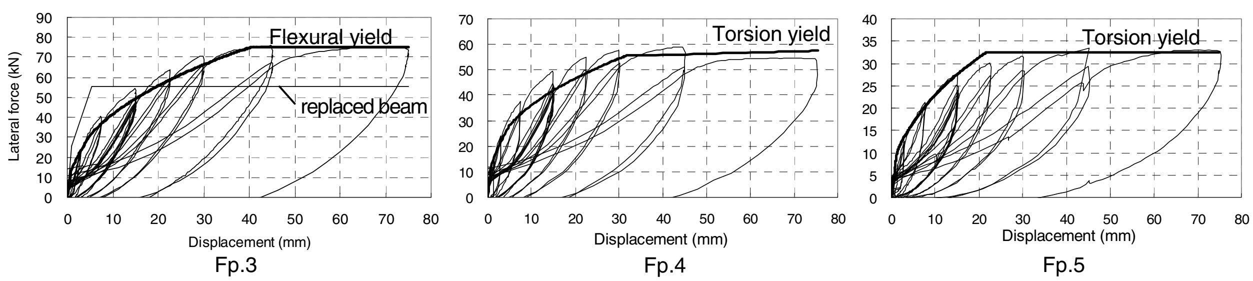

Fig. 14 : Estimation of load-deformation relation

Design procedure

The design method for the connection is to satisfy Eq. (1) by using Eqs. (4) and (5). The design procedure is as follows:

1. Assume the cross section and bar arrangement
2. Calculate the force under vertical loading
3. Consider extra coefficient α to be 1.5 by vertical earthquake motion
4. Estimate the load-deflection relation based on the macro model
5. Determine the design lateral force using the load-deflection relation at the earthquake deformation level
6. Take 1.5 times the force for the design safety factor
7. Examine Eq. (1). If NG, add shear reinforcement to satisfy the equation

CONCLUSION

The conclusions are as follows:

1. The punching shear strength can be calculated considering the following:
    - a） Shear strength of concrete section, connection plate, and effect of studs
    - b） Strength of the slab at the front and back of the column as the reinforced concrete section
    - c） Moment strength by shear force at the front and back of the column by concrete section and connection plate
    - d） Torsional moment strength of the column side slab
2. To set the adequate effective width of the torsion, load-deflection characteristics can be estimated with comparatively good accuracy.
3. Using the obtained results, the design method for the connection was proposed.

ACKNOWLEDGMENT

This study was funded by Grants-in-Aid for Scientific Research of JSPS. The opinions and findings do not necessarily represent those of the sponsor.

REFERENCES

1. Architectural Institute of Japan : AIJ Standard for Structural Calculation of Reinforced Concrete Structures －Based on Allowable Stress Concept－、1999
2. Yoshizaki S, Karino Y : Strength of Slab-Column Connections – Transferring Shear and Moment - , Transactions of the architectural institute of Japan, No.309, 1981.11
3. ACI-ASCE Committee 421: Shear Reinforcement for Slabs、ACI 421.1R-99
4. Japan Society of Civil Engineers : Standard Specifications for Concrete Structures、Japan Society of Civil Engineers publication committee
5. Hsu, T.T.C : Torsion of structural concrete – A summary on pure torsion, ACI, SP-18-6